

# QSpec: Speculative Decoding with Complementary Quantization Schemes\*

Juntao Zhao<sup>1,\*</sup> Wenhao Lu<sup>2,†</sup> Sheng Wang<sup>1,†</sup> Lingpeng Kong<sup>1</sup> Chuan Wu<sup>1</sup>

<sup>1</sup>The University of Hong Kong <sup>2</sup>Harbin Institute of Technology

Contact: [juntaozh@connect.hku.hk](mailto:juntaozh@connect.hku.hk)

## Abstract

Quantization has been substantially adopted to accelerate inference and reduce memory consumption of large language models (LLMs). While activation-weight joint quantization speeds up the inference process through low-precision kernels, we demonstrate that it suffers severe performance degradation on multi-step reasoning tasks, rendering it ineffective. We propose a novel quantization paradigm called QSPEC, which seamlessly integrates two complementary quantization schemes for speculative decoding. Leveraging nearly cost-free execution switching, QSPEC drafts tokens with low-precision, fast activation-weight quantization, and verifies them with high-precision weight-only quantization, effectively combines the strengths of both quantization schemes. Compared to high-precision quantization methods, QSPEC empirically boosts token generation throughput by up to  $1.64\times$  without any quality compromise, distinguishing it from other low-precision quantization approaches. This enhancement is also consistent across various serving tasks, model sizes, quantization methods, and batch sizes. Compared to state-of-art speculative decoding methods, our approach reuses weights and the KV cache, avoiding extra memory overhead while achieving up to  $1.55\times$  speedup in batched serving with a high acceptance rate. Furthermore, QSPEC offers a plug-and-play advantage without requiring any training. We believe that QSPEC demonstrates unique strengths for future deployment of high-fidelity quantization schemes, particularly in memory-constrained scenarios (*e.g.*, edge devices).

## 1 Introduction

Large language models (LLMs) have demonstrated remarkable abilities across various domains, including mathematics, coding, and planning (Shao et al., 2024b; Guo et al., 2024a; Huang et al., 2024). Nonetheless, their immense scales pose substantial challenges for deployment due to high memory and computational demands, especially in resource-limited scenarios (*e.g.*, inference on edge devices). Quantization has been an effective

compression technique to facilitate LLM inference with limited resources (Lin et al., 2024a; Ashkboos et al., 2024; Zhao et al., 2024b; Lin et al., 2024b). By converting high-precision values (*e.g.*, FP16) into their lower-precision counterparts (*e.g.*, INT4), quantization effectively lowers memory and computational requirements, allowing for larger serving batches and model sizes. Furthermore, the reduced memory footprint boosts token generation throughput by accelerating the typically memory-bound autoregressive decoding process (Zhao et al., 2024a).

Based on the quantized objects, recent quantization algorithms can be broadly classified into two categories: weight-only and WXAX: (1) Weight-only quantization, represented by W4A16 (Lin et al., 2024a), quantizes model weights to low precision (*e.g.*, 4-bit) for storage, and then dequantizes them to a higher precision (*i.e.*, FP16) during inference; (2) WXAX methods, such as W4A4 (Ashkboos et al., 2024; Zhao et al., 2024b) and W8A8 (Xiao et al., 2023), simultaneously quantize both weights and activations, and leverage low-precision hardware support for faster execution without dequantizing them to higher precision. Nevertheless, WXAX schemes generally suffer model performance degradation due to more low-precision activations used (as verified in Sec. 2). This poses a tough trade-off between efficacy and efficiency, raising the question:

*“Is there a quantization solution that boosts efficiency while avoiding performance degradation?”*

Considering the comparable performance claims on recent W4A4 methods (Zhao et al., 2024b; Ashkboos et al., 2024), we first contend that their conclusions are biased due to limited evaluation tasks, and W4A4 still experiences significant performance drops when compared to their higher-precision activation counterparts. Specifically, while W4A4 schemes such as Atom (Zhao et al., 2024b) and QuaRot (Ashkboos et al., 2024) perform well on general tasks, such as PIQA (Bisk et al., 2020), Winogrande (Sakaguchi et al., 2019) and ARC Clark et al. (2018), they demonstrate notable performance declines in multi-step reasoning, particularly on mathematical and coding benchmarks (Xiong et al., 2024; Guo et al., 2024b) (shown in Table 1). This raises concerns about the comprehensiveness of evaluation and emphasizes the

\*Corresponding author. †Equal contribution.

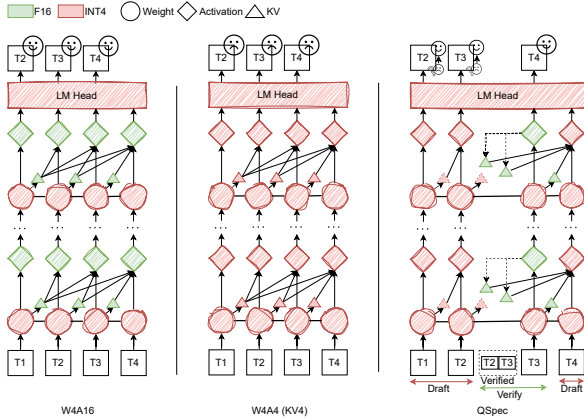


**Figure 1:** Diagrams of different 4-bit quantization schemes. **Left:** W4A16 uses 4-bit weight and 16-bit activation for inference. **Middle:** W4A4 further adopts 4-bit activation to utilize low-precision W4A4 kernels. **Right:** QSPEC accelerates W4A16 by drafting tokens with W4A4 and verifying them with W4A16, and applies KV cache overwriting for consistent memory consumption.

necessity of incorporating multi-step reasoning tasks into quantization assessment.

Then to answer the above question, we draw inspiration from Speculative Decoding (Leviathan et al., 2023; Chen et al., 2023), which combines rapid drafting of a small model with high-quality token generation of a larger model to boost throughput (*i.e.*, efficiency) without compromising performance (*i.e.*, efficacy). We propose a novel paradigm called QSPEC, which combines mixed-precision quantization execution to **tackle the trade-off between efficiency and efficacy while maintaining the memory usage of high-precision quantization**. Our key insight is that a single weight-quantized model can efficiently toggle two parallel quantization schemes: one with quantized activations and the other without, which we further empirically verify to produce highly similar tokens (Sec. 2.2). This observation unveils the potential for a synergistic approach combining both schemes. As illustrated in Figure 1, for a 4-bit weight-quantized model, we can leverage the faster yet lower-quality execution flow (*i.e.*, W4A4) to draft tokens, while verifying these drafted tokens with the higher-quality quantization flow (*i.e.*, W4A16) with negligible switching costs. Similar to speculative decoding, this ‘draft-verify’ mode with mixed quantization execution ensures high fidelity with the verifying flow. Differently, our approach re-utilizes the weights and high-precision KV cache, maintaining the memory overhead equivalent to that of the high-precision scheme alone, rather than the sum of both schemes in speculative decoding.

We evaluate the generation quality and end-to-end serving throughput of QSPEC against W4A4 and W4A16 schemes across multiple datasets, model sizes, quantization methods, and batch sizes. Empirically, QSPEC preserves memory consumption and generation quality

compared to W4A16, while offering a high acceptance rate and up to  $1.64\times$  higher token generation throughput, thereby mitigating the efficiency-efficacy trade-off of existing quantization methods. Notably, for multi-step reasoning tasks such as MATH (Hendrycks et al., 2021), QSPEC fully compensates for an up to 51.11% decline in generation quality observed with existing W4A4 methods. Furthermore, QSPEC provides plug-and-play compatibility without any training requirements, and can be seamlessly applied to any existing models, delivering superior performance with minimal effort.

In summary, our main contributions are as follows:

- We demonstrate that multi-step reasoning tasks can better capture the performance variations of quantization schemes than current evaluation protocols, and advocate for their incorporation for more comprehensive assessment.
- We validate and instantiate the feasibility of switching between two quantization schemes of a shared weight-quantized model, as well as their high token-level similarities, illuminating future development of quantization schemes.
- We propose QSPEC, the first quantization paradigm that synergizing two complementary weight-shared quantization schemes with speculative decoding, alleviating the efficiency-efficacy trade-off of quantization. We demonstrate its superior efficiency in quantized batch-serving compared to state-of-the-art speculative decoding approaches theoretically and empirically.
- Our empirical results reveal up to  $1.64\times$  acceleration without any quality sacrifice across diverse settings. Alongside consistent memory usage, these advantages promise QSPEC for high-fidelity quantization deployment, especially in memory-constrained scenarios.

## 2 Motivation

### 2.1 Compromised Performance of Activation Quantization

State-of-the-art (SOTA) activation-weight joint quantization methods, like Atom (Zhao et al., 2024b) and QuaRot (Ashkboos et al., 2024), achieve notable speed-ups with negligible performance loss compared to weight-only ones. However, we argue that this conclusion is skewed by the limited evaluation benchmarks, which fail to capture the negative impacts of activation quantization.

To substantiate this claim, we conduct experiments on Llama-3-8B-Instruct models (Dubey et al., 2024) quantized with W16A16, W4A16, and W4A4 methods across four task datasets: PIQA (Bisk et al., 2020), WikiText-2 (Merity et al., 2016), GSM8K (Cobbe et al., 2021), and MBPP (Austin et al., 2021). PIQA is a two-choice commonsense reasoning benchmark for physical knowledge,

**Table 1:** Performance of Atom-based quantization schemes with different weight and activation precision across diverse tasks. “Acc”, “PPL” and “EM” stand for accuracy, perplexity, and exact match, respectively, with arrows indicating their positive trends. “W16A16” refers to standard FP16 inference, where both weights and activations are represented in FP16 precision.

Task	Metric	W16A16	Quantization	
			Atom (W4A16)	Atom (W4A4)
WikiText-2	PPL ↓	7.73	7.87 (+0.15%)	8.58 (+0.85%)
PIQA (10-shot)	EM ↑	78.6	77.5 (-1.40%)	75.6 (-3.81%)
MBPP (0-shot)	EM ↑	42.0	41.5 (-1.19%)	30.5 (-27.38%)
GSM8K (8-shot)	EM ↑	79.0	73.4 (-7.09%)	54.2 (-31.39%)

evaluated using classification accuracy, while WikiText-2 comprises a collection of high-quality Wikipedia articles, assessed for language fluency via perplexity (Jelinek et al., 1977). Both are commonly adopted in current quantization evaluations. GSM8K includes diverse grade school mathematical problems, evaluated by “exact match” metrics; MBPP focuses on crowd-sourced Python programming challenges, assessed by accuracy. Unlike the former two benchmarks, both GSM8K and MBPP necessitate auto-regressive multi-step reasoning abilities. While these critical abilities are propelled by the rapid advancement in LLMs recently, they have not yet been widely integrated into mainstream quantization evaluation. As shown in Table 1, Atom-based quantization schemes show comparable performance to W16A16 across commonly adopted tasks such as on PIQA and WikiText-2, aligning with the claims in Zhao et al. (2024b). However, W4A4 suffers a nearly 30% average performance decline on complex reasoning tasks (*i.e.*, on MBPP and GSM8K), whereas W4A16 only experiences about 4%. This indicates that activation quantization leads to several times more performance degradation on multi-step reasoning tasks, despite the improved efficiency. Besides, the performance trend observed on multi-step reasoning tasks shows a stronger correlation with quantization precision than perplexity does, validating their adequacy in quantization evaluation.

In summary, activation quantization still incurs significant performance loss on more advanced multi-step reasoning tasks. This necessitates the inclusion of reasoning tasks in quantization evaluation for a more comprehensive assessment. On the other hand, this also underscores the demand for a quality-preserving yet efficient quantization paradigm.

## 2.2 High-Similarity Token Predictions

Despite the notable performance decline caused by activation quantization, we observe, more microscopically, high similarity in top-1 token predictions between quantization schemes with high and low precision activations. Specifically, we first employ Atom-based W4A16 greedy sampling to generate the golden token sequences for the

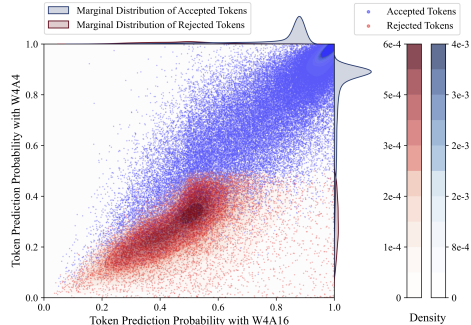


**Figure 2:** Scatter plot of token prediction probabilities for Atom-based W4A4 and W4A16 on GSM8K test set, along with their two-dimensional and marginal probability distributions. A striking similarity between the two quantization schemes is observed, laying the foundation of QSPEC.

GSM8K test set, obtaining the prediction probabilities for each top-1 answer token. Subsequently, we perform one Atom-based W4A4 forward pass (*i.e.*, prefill) on the concatenated input of each question and its corresponding golden answer to acquire the token probabilities as well. This allows us to assess the prediction discrepancy between W4A4 and W4A16. As illustrated in Figure 2, we observe that (1) the majority of token prediction probabilities of both W4A4 and W4A16 exceed 80%, and most of the tokens associated with high probabilities are accepted. (2) Compared to accepted tokens, the number of rejected ones is negligible, underscoring the high similarity between the two quantization methods. Combined with the analysis in Sec. 2.1, this can be interpreted that a small set of salient token variations can trigger a snowball effect of errors, especially on multi-step reasoning tasks where the subsequent steps are closely conditioned on the previous ones, akin to findings in Zhang et al. (2023), thus impairing the performance of the low-precision activation scheme. Prior studies indicate that low similarity leads to frequent token rejections, thereby diminishing the efficiency of speculative decoding (Leviathan et al., 2023). The observed high token-level similarity suggests that we could potentially restore the generation quality by detecting and correcting a limited number of generation errors incurred by activation quantization. This insight motivates us to propose a quantization-specific speculative decoding framework.

## 3 Method

Targeting an efficient quantization scheme without sacrificing performance or increasing memory consumption, we propose a new quantization paradigm called speculative decoding with complementary quantization execution (QSPEC). As shown in Figure 1, QSPEC employs a draft-verify pipeline for next-token prediction with varying activation precisions and shared low-precision quantized weights, instead of a single quantization scheme. The details are elaborated below, adhering to the core component

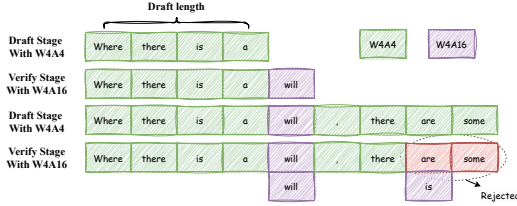


**Figure 3:** A mini-sample of QSPEC, where green, red, and purple tokens represent draft tokens, rejected tokens, and tokens generated directly by W4A16, respectively.

breakdown of regular speculative decoding (Leviathan et al., 2023).

### 3.1 QSpec

**Draft Phase.** Current LLMs typically utilize an autoregressive process for next-token prediction, where a new token is drawn from a probability distribution conditioned on all previously generated tokens. This process can be formulated as:

$$t_{i+1} \sim p_{i+1}(t) := \mathcal{M}(t_{i+1}|T_{\leq i}), \quad (1)$$

where  $\mathcal{M}$  denotes the model including the weight and activation configurations, while  $t_{i+1}$  and  $T_{\leq i}$  represent the next predicted token and the preceding token sequence  $(t_0, t_1, \dots, t_i)$ , respectively.

Compared with previous research (Leviathan et al., 2023; Chen et al., 2023), on one hand, we employ a weight-shared quantization scheme with low-precision activations, rather than one standalone small-sized model, to speculate the next  $\gamma$  tokens  $\hat{T}_{i+1:i+\gamma}$  and their associated distributions  $\hat{p}_{i+1:i+\gamma}(t)$ . In  $\hat{T}_{i+1:i+\gamma}$ , each token  $\hat{t}_j$  is sampled from  $\mathcal{M}_l(\hat{t}_j|T_{\leq i}, \hat{T}_{i+1:j-1})$ , where  $j \in [i+1, i+\gamma]$  and  $\mathcal{M}_l$  represent our quantized model executed with low-precision activation. On the other hand, our low-precision quantization scheme shares similar attributes as the draft model in Leviathan et al. (2023), as both can generate tokens rapidly, though with reduced quality.

**Verify Phase.** To compensate for the performance decline incurred by excessive quantization, we employ a high-precision weight-only quantization scheme to verify the proposed draft token sequence. This ensures that the final generation quality aligns with that of a high-precision activation quantization scheme. All drafted tokens are verified in parallel for higher efficiency.

Formally, the high-precision quantization scheme  $\mathcal{M}_h$  receives as input the concatenation of  $T_{\leq i}$  and  $\hat{T}_{i+1:i+\gamma}$ , producing high-quality prediction probabilities  $p_{i+1:i+\gamma+1}(t)$  through a single forward pass. Following this, an acceptance policy  $\mathcal{A}$ , which will be detailed later, is applied to rectify each drafted token sequentially. Once a token  $\hat{t}_{i+j}$  is rejected, all subsequent tokens are discarded, and token  $t_{i+j}$  is resampled according to the

**Table 2:** Comparison of individual quantization schemes, regular speculative decoding, and QSPEC across memory, computation, and generation aspects.

Method	Memory		Computation		Generation	
	Draft Weight	Draft KV	W4A4 Kernel	Draft-Verify	High Acceptance Rate	High Fidelity
W4A16	x	x	x	x	-	✓
W4A4	x	x	✓	x	-	x
Speculative Decoding	✓	✓	?	✓	?	✓
QSPEC	x	x	✓	✓	✓	✓

distribution  $p_{i+j}(t)$ . In the optimal scenario, all drafted tokens from the low-precision quantized model are accepted by the high-precision model. Subsequently, an additional token  $t_{i+\gamma+1}$  is sampled from  $p_{i+\gamma+1}(t)$ . From this point, a new draft-verify cycle commences, persisting until the sequence is finalized.

**Acceptance Policy.** To maintain high reproducibility, both low-precision and high-precision activation quantization schemes employ greedy decoding. This means that one drafted tokens  $\hat{t}_{i+j}$  is accepted as  $t_{i+j}$  only when the top-1 tokens from  $p_{i+j}$  and  $\hat{p}_{i+j}$  coincide; otherwise, this token is rejected. Nonetheless, we claim that alternative strategies, as outlined in Leviathan et al. (2023), can be directly applied to our method due to the similarities in the framework. Figure 3 illustrates a mini-sample of this cycle with the draft token length  $\gamma = 4$ . The model initially speculates four tokens using W4A4 scheme. Subsequently, adhering to a predefined acceptance policy, it accepts all drafted tokens after verifying them through the W4A16 scheme. In the second loop, however, only the first two tokens are accepted. A new token “is” is directly derived from the prediction probability of W4A16 scheme, and another draft-verify cycle will commence from the ninth token.

**KV Cache Overwriting.** To further reduce memory consumption, QSPEC overwrites KV caches of low-precision activation quantization with those of high-precision method. Specifically, compared to W4A4, W4A16 is expected to yield a higher quality FP16 KV cache due to higher activation precision. Alongside the shared weights, this naturally allows overwriting the low-quality KV caches generated by W4A4 with those from W4A16 for accepted tokens after each validation phase. This enables W4A4 to condition on high-quality KV caches for subsequent autoregressive generation, and saves the memory occupation of W4A4 KV caches, despite requiring negligible buffer space for temporarily storing. To some extent, this operation aligns with the settings of attention kernels in prior works (Zhao et al., 2024b; Shao et al., 2024a; Ashkboos et al., 2024), where INT4 KV caches are typically dequantized to FP16 before or during precision-sensitive attention operations to ensure accurate computations. Note that *KV compression* (Hooper et al., 2024; Kang et al., 2024) is fully orthogonal to our method, e.g., it is also possible to use 4-bit KV cache for W4A16.

As shown in Table 2, we compare QSPEC against individual quantization configurations (i.e., W4A4 and

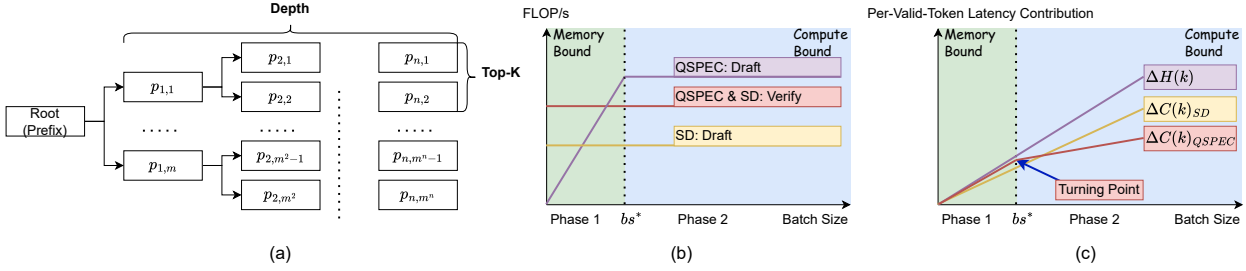


**Figure 4:** Analysis of QSPEC advantages: (a) Tree-structured drafting architecture, (b) Roofline model showing computational efficiency transitions (memory-bound  $\rightarrow$  compute-bound) with batch size scaling, and (c) Per-valid-token latency composition comparing the change of extra computational overhead and accepted token numbers with scaling batch size. SD denotes tree-structured speculative decoding.

W4A16) and speculative decoding in terms of memory, computation, and generation. QSPEC provides four key benefits:

- (1) Memory-Efficient. By sharing weights and overwriting KV caches, QSPEC incurs memory costs on par with standalone high-precision activation quantization.
- (2) No Efficiency-Efficacy Trade-off. QSPEC leverages speculative decoding to boost efficiency while preserving output quality, avoiding the compromises seen in conventional quantization.
- (3) Plug-and-Play Compatibility. QSPEC requires only an acceptance policy and a cache-overwriting step, requiring no additional training or classifiers. Hence, it can be quickly integrated into existing quantization pipelines.
- (4) High Acceptance Rate. Common weights and KV cache overwriting ensure consistent predictions, leading to a high rate of token acceptance.

### 3.2 Advantages of High Acceptance Rate

A key advantage of QSPEC lies in its superior acceptance rate. While state-of-the-art speculative decoding approaches such as EAGLE Li et al. (2024a) and Medusa Cai et al. (2024) rely on compressed draft models and tree-structured drafting to balance speed and accuracy, QSPEC achieves high performance without such compromises. We analyze how QSPEC demonstrates superior performance compared to these methods in quantized settings below.

**Tree-Structured Drafting.** As shown in Figure 4 (a), tree-structured drafting (Chen et al., 2024; Miao et al., 2024; Li et al., 2024a,b) is a widely adopted technique to improve acceptance rates in speculative decoding. Instead of generating a single draft token at a time using the draft model  $\mathcal{M}_d$ ,  $\mathcal{M}_d$  select  $k$  (i.e., topk) tokens and infers  $\gamma$  times to form a draft tree with depth  $\gamma$ . The target model  $\mathcal{M}$  then verifies the tokens using masked tree attention, with the exact verification strategy depending on the sampling method (Cai et al., 2024; Miao et al., 2024). Under greedy sampling, the highest-probability token at each position is selected, forming the longest branch with the common prefix as the accepted sequence. In this tree, root node presents the past sequence, any token  $t_i$  has a path from the root node  $r$  to  $t_i$ , denoted by  $Path(r, t_i)$ , consisting of ancestors  $a_1, \dots, a_j$ .

**Expected average accepted token number.** Let  $p_a(t)$  be the probability of accepting a token  $t$ . The average accepted token number is given by:

$$H(k) := \sum_l^\gamma \sum_{i=1}^{k^l} \prod_{j \in Path(r, t_i)} p_a(a_j), \quad (2)$$

where  $k$  controls the tree’s branching factor (width). Larger  $k$  indicates larger expected token acceptance. When  $k = 1$ , this method reduces to standard speculative decoding.

**Cost Analysis.** Denote by  $C_d(\cdot)$  and  $C_p(\cdot)$  the computation cost for draft and verify, The first argument indicates the number of sequences, and the second argument is the prefix sequence length. For a prefix with length  $s$ , we have *per-valid-token* cost  $v$  by dividing the total cost by the number of accepted tokens:

$$v = \frac{\overbrace{C_d(1; s) + \dots + C_d(k^{\gamma-1}; s + \gamma - 1)}^{\text{Drafting cost}} + \overbrace{C_p(k^{\gamma-1}; s + \gamma)}^{\text{Verify cost}}}{\underbrace{H(k)}_{\text{Accepted tokens}}} \sim \frac{C(k)}{H(k)}. \quad (3)$$

**Batch serving efficiency of QSpec.** From Equation 3, efficient tree-structured drafting benefits from less extra computational overhead  $\Delta C(k)_{SD}$  against acceptance rate gains  $\Delta H(k)$ , as illustrated in Figure 4(c). QSPEC advances this paradigm in batched serving. As shown in Figure 4(b), QSPEC employs W4A4 quantization for drafting. While initially exhibiting two limitations - suboptimal hardware utilization during the drafting and higher computational costs compared to small/pruned models - these challenges diminish with increased batch sizes. Beyond critical batch size  $bs^*$ , QSPEC’s draft phase transits from memory-bound to compute-bound, achieving superior FLOP/s with low-precision. Also, by eschewing penalties for acceptance rate maintenance, QSPEC reduces costs by a factor of  $k$ . As a result, in Figure 4(c),  $\Delta C(k)_{QSPEC}$  curve maintains a consistently shallower slope than  $\Delta C(k)_{SD}$  for  $bs > bs^*$ , enabling higher token generation throughput. This observation applies to both static (e.g., SpecInfer (Miao et al., 2024), Sequoia (Chen et al., 2024)) and dynamic (Wang et al., 2024; Li et al., 2024b) tree-structured drafting methods, all of which exhibit similar behaviors.

## 4 Experiments

Our evaluation answers three key questions:

- Q1: Does QSPEC preserve the quality of high-precision weight-only quantization? (Sec. 4.2)
- Q2: Does QSPEC accelerate high-precision weight-only quantization methods and surpass SOTA speculative decoding method in quantized scenarios? (Sec.4.3)
- Q3: How do various factors (*e.g.*, quantization method, sequence length) influence QSPEC’s acceptance rate and acceleration performance? (Sec. 4.4)

### 4.1 General Setup

**Benchmarks.** We assess QSPEC with two primary criteria: (1) generation fidelity and (2) end-to-end serving speedup. For fidelity evaluation, we adopt not only traditional tasks, including PIQA (500, 10-shot) (Bisk et al., 2020), WinoGrande (500, 5-shot) (Sakaguchi et al., 2019), and WikiText2 (Merity et al., 2016), but also challenging multi-step reasoning tasks such as GSM8K (All, 8-shot) (Cobbe et al., 2021), MATH (All, 4-shot) (Hendrycks et al., 2021), MBPP (200, 0-shot) (Austin et al., 2021), and HumanEval (All, 0-shot) (Chen et al., 2021). To measure the acceleration, we use all the above reasoning tasks and two additional chatbot datasets, namely ShareGPT (RyokoAI, 2021) and LMsys-1K (Zheng et al., 2023). Due to space constraints, we present results for GSM8K, HumanEval, and LMsys-1K in the main text, with remaining results detailed in the Appendix A. Following the setup of Atom (Zhao et al., 2024b), we randomly sampled the dataset for the request prompts to reduce the workload. Due to memory limitations, we vary the batch size from 8 to 32 and serve all requests in a first-come, first-served (FCFS) manner. Once any request is finished, we refill the batch, adhering to the continuous batching approach of ORCA (Yu et al., 2022). All experiments use greedy sampling for token generation.

**Models.** To assess the effectiveness and scalability of our approach, we conduct experiments using multiple models from the Llama family (Touvron et al., 2023; Dubey et al., 2024) with varying scales and capacities: Llama3.2-3b, Llama2-7b, Llama3-8b-instruct, and Llama2-13b.

**Implementations.** All experiments are performed on a node equipped with four NVIDIA L20 GPUs (48GB HBM each) running CUDA 12.5. To demonstrate the versatility of QSPEC, we implement two SOTA 4-bit quantization methods, namely Atom (Zhao et al., 2024b) and QuaRot (Ashkboos et al., 2024). For W4A16 configurations, we incorporate AWQ-style (Lin et al., 2024a) weight dequantization logic for runtime inference. We select Atom to showcase the acceleration of QSPEC. We use these Group-wise quantization schemes with a group size of 128. With the draft token length  $\gamma$  as 3, we simulate the performance of QSPEC by initially employing

fake quantization to fully emulate the execution flow, encompassing both the draft and verify stages of QSPEC. Subsequently, we replay the collected traces with real kernel execution to accurately reproduce the latency.

**Baselines.** We evaluate QSPEC against baseline quantization configurations: W4A4, W4A16, and W16A16. For comparison with SOTA speculative decoding approaches, we include EAGLE (Li et al., 2024a), which employs a pruned draft model with tree-structured speculative decoding. In our quantized experiments, we utilize FP16 precision for the EAGLE draft model and EAGLE-Quant (W4A16) for the target model. This choice was necessitated by two factors: (1) the official EAGLE quantization implementation (fast-gpt) lacks efficient batching support, and (2) applying GPTQ quantization to the EAGLE draft model resulted in substantial degradation of the acceptance rate.

### 4.2 Fidelity Evaluation

**QSpec effectively maintains the generation quality of W4A16, whereas W4A4 does not.** As listed in Table 3, with the draft verification of W4A16, QSPEC exhibits only minimal performance fluctuations compared to W4A16. This negligible variation may stem from the nondeterministic algorithms of PyTorch (PyTorch Contributors, 2024) or occasional cases where two tokens have the same maximum prediction probability. In contrast, W4A4 experiences a substantial performance decline exceeding 10% across most tasks, with the reduction becoming more pronounced as task difficulty increases. For instance, compared to GSM8K and MBPP, the performance drop for W4A4 is much greater on the more challenging MATH and HumanEval tasks, showing declines of 51.11% and 38.73%, respectively. On the other hand, this also highlights the higher sensitivity of multi-step reasoning tasks to the negative effects of quantization compared to regular tasks, such as WikiText-2 and WinoGrande. This observation aligns with our earlier analysis in Sec. 2, encouraging incorporating multi-step reasoning tasks into quantization evaluation.

### 4.3 Acceleration Evaluation

**QSpec exhibits a substantial efficiency boost compared to W4A16.** In Table 4, we present the token generation throughput for both QSPEC and W4A16 across different model sizes, quantization configurations, and batch sizes on diverse datasets. On average, QSPEC achieves a throughput increase of  $1.38\times$  over W4A16 across all settings, with a peak improvement of  $1.64\times$ .

**Larger models tend to yield better speedup ratios.** We find a gradually-increasing acceleration as the base model scales up. This overall upward trend indicates a promising outlook for our approach with larger models, although further experiments are needed for confirmation.

**Table 3:** Performance of different quantization methods across multiple general and reasoning benchmarks: PIQA, WinoGrande, GSM8K, MATH, MBPP, and HumanEval. The quality degradation ratio is calculated by  $\frac{W4A4}{W4A16} - 1$ .

Method	Quantization	WikiText-2 PPL ↓	PIQA EM (%) ↑	WinoGrande EM (%) ↑	GSM8K EM (%) ↑	MATH EM (%) ↑	MBPP Pass@1 (%) ↑	HumanEval Pass@1 (%) ↑
Atom	W16A16	7.73	76.8	61.4	76.2	24.9	42.5	53.0
	W4A16	7.87	74.8	62.0	73.4	24.3	42.0	52.4
	QSPEC	7.87	75.0	62.0	73.4	24.3	40.5	52.4
	W4A4	8.6 (+9.58%)	65.8 (-12.03%)	56.2 (-9.35%)	54.7 (-25.47%)	15.5 (-36.21%)	33.0 (-21.43%)	31.7 (-39.50%)
QuaRot	W16A16	7.73	76.8	61.4	76.2	24.9	42.5	53.0
	W4A16	8.58	74.2	59.4	70.5	24.7	40.0	45.7
	QSPEC	8.58	74.4	59.2	71.0	24.7	40.5	47.6
	W4A4	10.2 (+19.24%)	62.6 (-15.63%)	53.8 (-9.43%)	42.0 (-40.43%)	12.3 (-51.11%)	28.5 (-28.75%)	28.0 (-38.73%)

**Table 4:** Comparison of token generation throughput across different model sizes, quantization configurations, and batch sizes for various datasets. All values are measured in token/s. "Avg." denotes the average speedup ratio for the corresponding row or column. "†" indicates the failure of W4A16 kernels to support the configuration. W16A16 results (when OOM) are collected using pipeline parallelism Harlap et al. (2018) with multiple cards.

Model	Method	Batch	GSM8K	HumanEval	LMsys-1k
3B	W16A16	8	511.1	647.2	711.2
		16	666.5	948.3	1126.4
		32	833.4	1111.6	1553.3
	W4A4	8	804.7	892.6	990.3
		16	1109.1	1289.8	1581.0
		32	1424.3	1488.2	2194.4
	W4A16	8	420.0	535.7	559.8
		16	578.5	804.4	925.8
		32	726.3	954.4	1336.4
	QSPEC	8	594.1 (1.41×)	723.6 (1.35×)	738.8 (1.32×)
		16	811.5 (1.40×)	1042.1 (1.30×)	1171.4 (1.27×)
		32	1030.4 (1.42×)	1248.5 (1.31×)	1576.0 (1.18×)
Avg.		1.41×	1.32×	1.25×	
7B	W16A16	8	213.4	316.7	285.3
		16	290.3	505.1	441.6
		32	340.9	663.6	564.2
	W4A4	8	349.5	471.2	419.4
		16	496.6	749.5	642.6
		32	620.0	1043.9	865.5
	W4A16	8	165.0	240.2	220.2
		16	231.8	407.3	358.0
		32	268.9	555.9	470.1
	QSPEC	8	253.7 (1.54×)	350.9 (1.46×)	310.3 (1.41×)
		16	359.8 (1.55×)	555.2 (1.36×)	473.1 (1.32×)
		32	441.8 (1.64×)	749.4 (1.35×)	628.4 (1.34×)
Avg.		1.58×	1.39×	1.36×	
13B	W16A16	8	121.9	182.0	160.1
		16	169.6	291.0	243.0
		32	202.4	423.5	334.2
	W4A4	8	194.7	261.5	228.2
		16	288.3	424.9	348.4
		32	369.8	665.4	508.8
	W4A16	8	94.8	140.0	127.9
		16	136.1	236.9	207.2
		32	†	365.5	287.4
	QSPEC	8	148.2 (1.56×)	201.2 (1.44×)	174.0 (1.36×)
		16	212.8 (1.56×)	323.3 (1.36×)	266.9 (1.29×)
		32	266.6 (†)	483.0 (1.32×)	379.3 (1.32×)
Avg.		1.56×	1.37×	1.32×	

Due to resource limitations, this will be addressed in future work.

**Latency composition.** As illustrated in Figure 5, we compute the per-valid-token latency by dividing the

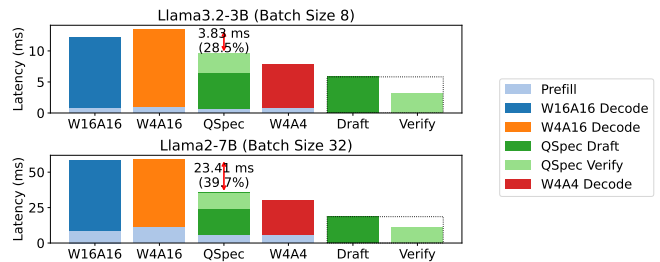


**Figure 5:** Per-valid-token latency decomposition for different methods. The latency of QSPEC is further decomposed into draft and verify categories for details.

**Table 5:** Performance comparison of EAGLE-Quant, QSPEC, W4A16, and W4A4 on Llama-2-7b-chat-hf across different batch sizes and benchmarks. "OOM" indicates out-of-memory. Better cases for QSPEC or EAGLE is marked in gray. In the case of batch size=8, the speedup ratio of QSPEC compared to EAGLE is indicated in parentheses next to the data points.

Method	Batch Size	GSM8K (8-shot)	HumanEval (0-shot)	LMsys-1k
EAGLE	1	65.81	49.15	71.29
	8	140.16	136.86	167.57
	16	OOM	OOM	OOM
QSPEC	1	51.25	54.22	56.14
	8	208.95 (1.49×)	185.99 (1.36×)	260.48 (1.55×)
	16	292.82	255.11	463.35
W4A16	1	59.80	72.04	72.27
	8	146.34	163.54	213.66
	16	190.09	211.49	371.38
W4A4	1	64.79	73.47	71.55
	8	284.84	256.54	393.12
	16	401.77	330.71	713.67

total latency by only the number of accepted tokens before averaging on all evaluation datasets. Notably, QSPEC achieves remarkable latency savings ranging from 28.5% to 39.7%. Besides, the per-token latency is further decomposed into two parts: draft and verify. Clearly, the primary gains of QSPEC arise from the rapid drafting capability and the reduced latency achieved through the parallel verification of multiple tokens.

**Memory and batching efficiency over speculative decoding.** Table 4.3 compares QSPEC and EAGLE on Llama-2-7b-chat-hf. EAGLE delivers optimal performance for single-sequence inputs (batch size=1). However, its efficiency degrades as the batch size grows (8 and 16). This observation aligns with our earlier analysis in Sec. 3.2: EAGLE’s tree-structured drafting mechanism, designed to reconcile discrepancies between the draft and target

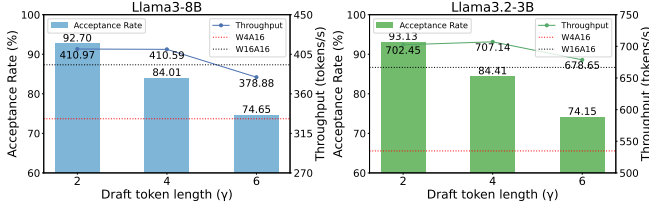


**Figure 6:** Acceptance rate and throughput of Llama3.2-3b (batch size 8) and Llama3-8b-instruct (batch size 16) with respect to the draft token length  $\gamma$ .

**Table 6:** Ablation study comparing acceptance rates (%) across base quantization methods using QSPEC.

Quantization Method	ShareGPT	MATH (4-shot)	MBPP (0-shot)
Atom	83.8	89.4	88.6
QuaRot	81.6	88.9	85.4

models, introduces additional latency that reduces the gains from higher acceptance rates in batched serving under quantization. Furthermore, the increasing key-value (KV) storage of EAGLE’s draft model leads to out-of-memory (OOM) issues at batch size 16. In contrast, QSPEC demonstrates superior scalability and memory efficiency.

#### 4.4 Ablation Study

**Ablation on draft token length.** To assess parameter sensitivity, we vary the draft token lengths  $\gamma$ , the sole hyper-parameter of QSPEC, from 2 to 6 across all the benchmarks using Llama3.2-3b and Llama3-8b-instruct models. As depicted in Figure 6, an increase in  $\gamma$  leads to a gradual decline in the token acceptance rate, since all subsequent tokens are discarded once a token is rejected. Nevertheless, even at  $\gamma = 6$ , the token acceptance rate remains relatively high, approximately 74%, compared to 28 ~ 58% in 160m-7b draft-target model pair under  $\gamma = 5$  in conventional speculative decoding (Liu et al., 2024). Additionally, a consistent improvement in throughput is observed compared to W4A16, indicating the robustness of QSPEC with respect to  $\gamma$ . More comprehensive comparison is provided in Appendix A.2.

**Ablation on base quantization method.** As shown in Table 6, QSPEC consistently achieves high acceptance rates across diverse quantization methods and datasets.

## 5 Related work

**Quantization** is a common technique for deploying LLMs on resource-limited scenarios. Broadly, recent quantization algorithms can be classified into two categories: weight-only W4A16 and weight-activation joint W4A4. Notably, AWQ (W4A16) (Lin et al., 2024a) redistributes the quantization burden by scaling salient weight channels to protect them from degradation. In contrast, W4A4 aggressively quantizes activations to leverage low-precision hardware for improved speed at the cost of model quality degradation. To address this challenge, Atom (Zhao et al., 2024b) proposes reordering outlier channels in the activa-

tion through offline profiling. Similarly, QuaRot (Ashkboos et al., 2024) employs Hadamard matrices to apply computational invariance on weights. Despite these advancements, our observations indicate that W4A4 methods still exhibit substantial degradation compared to weight-only quantization approaches across multi-step reasoning tasks. Works such as W4A8 (Lin et al., 2024b) and adaptive quantization (Zhao et al., 2024a; Dong et al., 2024) seek to identify an optimal trade-off point. However, these methods struggle to fully preserve the generation quality associated with higher precision.

**Speculative Decoding** leverages a draft model to generate candidate tokens, which are then validated by a target model (Leviathan et al., 2023). Recent research has primarily focused on improving the acceptance rate and generation speed of candidate tokens. SpecInfer (Miao et al., 2024) introduces a boost-tuned small language model to generate candidate tokens in tree structures, enabling single-pass verification. In contrast, EAGLE (Li et al., 2024a) adopts an aggressive pruning strategy for the draft model’s architecture, allowing penultimate layer feature prediction with minimal computational overhead. Self-speculative decoding, a subset of this technique, employs a single model for both draft generation and verification. LayerSkip (Elhoushi et al., 2024) introduces a training methodology for early exit with layer drop, subsequently verifying partially generated tokens through full model inference. Medusa (Cai et al., 2024) augments the original LLM with additional heads atop the final hidden state while relaxing the acceptance policy. However, these approaches inevitably require retraining of the original model, which can be computationally expensive and time-consuming. We further demonstrate their deficiency in batched serving under quantization scenario.

## 6 Conclusion

In this paper, we begin by validating that multi-step reasoning tasks can capture performance degradation incurred by activation quantization more sensitively and consistently than current evaluation protocols, advocating for their incorporation for a more comprehensive assessment. With observed high token-level similarities, we introduce QSPEC, a novel quantization paradigm that seamlessly synergizes two complementary weight-shared quantization schemes with speculative decoding. Empirically, QSPEC achieves up remarkable acceleration without any quality sacrifice across diverse settings and baselines. Alongside consistent memory consumption and a plug-and-play property, these advantages distinguish QSPEC from any existing solution, promising it for high-fidelity quantization deployment, particularly in memory-constrained scenarios.

## 7 Impact Statement

This paper introduces QSPEC, a novel quantization paradigm that synergistically combines complementary

quantization schemes for speculative decoding to enhance computational efficiency while preserving model fidelity. The impact of QSPEC is twofold.

From an academic perspective, QSPEC establishes a new paradigm that decouples speed acceleration from quality preservation—a longstanding trade-off in prior quantization research. By enabling independent optimization of these objectives, our work addresses critical challenges in quantization design—particularly under modern training regimes where improved model convergence and higher parameter utilization efficiency amplify the severity of precision degradation caused by quantization [Kumar et al. \(2024\)](#).

For industry applications, QSPEC provides a practical pathway to accelerate inference without compromising output quality through efficient low-precision kernels. This advancement challenges hardware vendors to reconsider architectural support for low-precision execution, including specialized instruction set architectures (ISAs) and memory subsystems. The plug-and-play nature of QSPEC further facilitates seamless integration into existing deployments of quantized models on edge devices, lowering barriers to adoption.

We identify no direct adverse societal impacts, as our work focuses on optimizing computational efficiency for language model serving systems. By reducing resource requirements, QSPEC could broaden access to high-performance AI infrastructure, thereby contributing to more sustainable and scalable deployments of language technologies.

## References

- Ainslie, J., Lee-Thorp, J., de Jong, M., Zemlyanskiy, Y., Lebrón, F., and Sanghai, S. Gqa: Training generalized multi-query transformer models from multi-head checkpoints, 2023. URL <https://arxiv.org/abs/2305.13245>.
- Ashkboos, S., Mohtashami, A., Croci, M. L., Li, B., Jaggi, M., Alistarh, D., Hoefler, T., and Hensman, J. Quarot: Outlier-free 4-bit inference in rotated llms, 2024. URL <https://arxiv.org/abs/2404.00456>.
- Austin, J., Odena, A., Nye, M., Bosma, M., Michalewski, H., Dohan, D., Jiang, E., Cai, C., Terry, M., Le, Q., and Sutton, C. Program synthesis with large language models, 2021. URL <https://arxiv.org/abs/2108.07732>.
- Bisk, Y., Zellers, R., Bras, R. L., Gao, J., and Choi, Y. Piqa: Reasoning about physical commonsense in natural language. In *Thirty-Fourth AAAI Conference on Artificial Intelligence*, 2020.
- Cai, T., Li, Y., Geng, Z., Peng, H., Lee, J. D., Chen, D., and Dao, T. Medusa: Simple llm inference acceleration framework with multiple decoding heads, 2024. URL <https://arxiv.org/abs/2401.10774>.
- Chen, C., Borgeaud, S., Irving, G., Lespiau, J.-B., Sifre, L., and Jumper, J. Accelerating large language model decoding with speculative sampling. *arXiv preprint arXiv:2302.01318*, 2023.
- Chen, M., Tworek, J., Jun, H., Yuan, Q., de Oliveira Pinto, H. P., Kaplan, J., Edwards, H., Burda, Y., Joseph, N., Brockman, G., Ray, A., Puri, R., Krueger, G., Petrov, M., Khlaaf, H., Sastry, G., Mishkin, P., Chan, B., Gray, S., Ryder, N., Pavlov, M., Power, A., Kaiser, L., Bavarian, M., Winter, C., Tillet, P., Such, F. P., Cummings, D., Plappert, M., Chantzis, F., Barnes, E., Herbert-Voss, A., Guss, W. H., Nichol, A., Paino, A., Tezak, N., Tang, J., Babuschkin, I., Balaji, S., Jain, S., Saunders, W., Hesse, C., Carr, A. N., Leike, J., Achiam, J., Misra, V., Morikawa, E., Radford, A., Knight, M., Brundage, M., Murati, M., Mayer, K., Welinder, P., McGrew, B., Amodei, D., McCandlish, S., Sutskever, I., and Zaremba, W. Evaluating large language models trained on code. 2021.
- Chen, Z., May, A., Svirschevski, R., Huang, Y., Ryabinin, M., Jia, Z., and Chen, B. Sequoia: Scalable, robust, and hardware-aware speculative decoding, 2024. URL <https://arxiv.org/abs/2402.12374>.
- Clark, P., Cowhey, I., Etzioni, O., Khot, T., Sabharwal, A., Schoenick, C., and Tafjord, O. Think you have solved question answering? try arc, the ai2 reasoning challenge. *arXiv:1803.05457v1*, 2018.
- Cobbe, K., Kosaraju, V., Bavarian, M., Chen, M., Jun, H., Kaiser, L., Plappert, M., Tworek, J., Hilton, J., Nakano, R., Hesse, C., and Schulman, J. Training verifiers to solve math word problems, 2021. URL <https://arxiv.org/abs/2110.14168>.
- Dong, S., Cheng, W., Qin, J., and Wang, W. Qaq: Quality adaptive quantization for llm kv cache. *ArXiv*, abs/2403.04643, 2024. URL <https://api.semanticscholar.org/CorpusID:268264510>.
- Dubey, A., Jauhri, A., Pandey, A., Kadian, A., Al-Dahle, A., Letman, A., Mathur, A., Schelten, A., Yang, A., Fan, A., et al. The llama 3 herd of models. *arXiv preprint arXiv:2407.21783*, 2024.
- Elhoushi, M., Shrivastava, A., Liskovich, D., Hosmer, B., Wasti, B., Lai, L., Mahmoud, A., Acun, B., Agarwal, S., Roman, A., Aly, A., Chen, B., and Wu, C.-J. Layerskip: Enabling early exit inference and self-speculative decoding. *ArXiv*, abs/2404.16710, 2024. URL <https://api.semanticscholar.org/CorpusID:269362647>.
- Guo, D., Zhu, Q., Yang, D., Xie, Z., Dong, K., Zhang, W., Chen, G., Bi, X., Wu, Y., Li, Y. K., Luo, F., Xiong, Y., and Liang, W. Deepseek-coder: When the large language model meets programming – the rise of code intelligence, 2024a. URL <https://arxiv.org/abs/2401.14196>.

- Guo, H., Liu, Z., Zhang, Y., and Wang, Z. Can large language models play games? a case study of a self-play approach. *arXiv preprint arXiv:2403.05632*, 2024b.
- Harlap, A., Narayanan, D., Phanishayee, A., Seshadri, V., Devanur, N., Ganger, G., and Gibbons, P. Pipedream: Fast and efficient pipeline parallel dnn training, 2018. URL <https://arxiv.org/abs/1806.03377>.
- Hendrycks, D., Burns, C., Kadavath, S., Arora, A., Basart, S., Tang, E., Song, D., and Steinhardt, J. Measuring mathematical problem solving with the math dataset. *NeurIPS*, 2021.
- Hooper, C., Kim, S., Mohammadzadeh, H., Mahoney, M. W., Shao, Y. S., Keutzer, K., and Ghohami, A. Kvquant: Towards 10 million context length llm inference with kv cache quantization. *ArXiv*, abs/2401.18079, 2024. URL <https://api.semanticscholar.org/CorpusID:267335271>.
- Huang, X., Liu, W., Chen, X., Wang, X., Wang, H., Lian, D., Wang, Y., Tang, R., and Chen, E. Understanding the planning of llm agents: A survey. *arXiv preprint arXiv:2402.02716*, 2024.
- Jelinek, F., Mercer, R. L., Bahl, L. R., and Baker, J. K. Perplexity—a measure of the difficulty of speech recognition tasks. *The Journal of the Acoustical Society of America*, 62(S1):S63–S63, 1977.
- Kang, H., Zhang, Q., Kundu, S., Jeong, G., Liu, Z., Krishna, T., and Zhao, T. Gear: An efficient kv cache compression recipe for near-lossless generative inference of llm. *ArXiv*, abs/2403.05527, 2024. URL <https://api.semanticscholar.org/CorpusID:268297231>.
- Kumar, T., Ankner, Z., Spector, B. F., Bordelon, B., Muennighoff, N., Paul, M., Pehlevan, C., Ré, C., and Raghunathan, A. Scaling laws for precision, 2024. URL <https://arxiv.org/abs/2411.04330>.
- Leviathan, Y., Kalman, M., and Matias, Y. Fast inference from transformers via speculative decoding, 2023. URL <https://arxiv.org/abs/2211.17192>.
- Li, Y., Wei, F., Zhang, C., and Zhang, H. Eagle: Speculative sampling requires rethinking feature uncertainty, 2024a. URL <https://arxiv.org/abs/2401.15077>.
- Li, Y., Wei, F., Zhang, C., and Zhang, H. Eagle-2: Faster inference of language models with dynamic draft trees, 2024b. URL <https://arxiv.org/abs/2406.16858>.
- Lin, J., Tang, J., Tang, H., Yang, S., Chen, W.-M., Wang, W.-C., Xiao, G., Dang, X., Gan, C., and Han, S. Awq: Activation-aware weight quantization for llm compression and acceleration, 2024a. URL <https://arxiv.org/abs/2306.00978>.
- Lin, Y., Tang, H., Yang, S., Zhang, Z., Xiao, G., Gan, C., and Han, S. Qserve: W4a8kv4 quantization and system co-design for efficient llm serving, 2024b. URL <https://arxiv.org/abs/2405.04532>.
- Liu, X., Hu, L., Bailis, P., Cheung, A., Deng, Z., Stoica, I., and Zhang, H. Online speculative decoding, 2024. URL <https://arxiv.org/abs/2310.07177>.
- Merity, S., Xiong, C., Bradbury, J., and Socher, R. Pointer sentinel mixture models, 2016.
- Miao, X., Oliaro, G., Zhang, Z., Cheng, X., Wang, Z., Zhang, Z., Wong, R. Y. Y., Zhu, A., Yang, L., Shi, X., Shi, C., Chen, Z., Arfeen, D., Abhyankar, R., and Jia, Z. Specinfer: Accelerating large language model serving with tree-based speculative inference and verification. In *Proceedings of the 29th ACM International Conference on Architectural Support for Programming Languages and Operating Systems, Volume 3*, ASPLOS '24. ACM, April 2024. doi: 10.1145/3620666.3651335. URL <http://dx.doi.org/10.1145/3620666.3651335>.
- PyTorch Contributors. Reproducibility. <https://pytorch.org/docs/stable/notes/randomness.html>, 2024. PyTorch Documentation, Accessed: January 2024.
- RyokoAI. Sharegpt52k, 2021.
- Sakaguchi, K., Bras, R. L., Bhagavatula, C., and Choi, Y. Winogrande: An adversarial winograd schema challenge at scale, 2019. URL <https://arxiv.org/abs/1907.10641>.
- Shao, W., Chen, M., Zhang, Z., Xu, P., Zhao, L., Li, Z., Zhang, K., Gao, P., Qiao, Y., and Luo, P. Omniquant: Omnidirectionally calibrated quantization for large language models, 2024a. URL <https://arxiv.org/abs/2308.13137>.
- Shao, Z., Wang, P., Zhu, Q., Xu, R., Song, J., Bi, X., Zhang, H., Zhang, M., Li, Y. K., Wu, Y., and Guo, D. Deepseekmath: Pushing the limits of mathematical reasoning in open language models, 2024b. URL <https://arxiv.org/abs/2402.03300>.
- Touvron, H., Martin, L., Stone, K., Albert, P., Almahairi, A., Babaei, Y., Bashlykov, N., Batra, S., Bhargava, P., Bhosale, S., Bikel, D., Blecher, L., Ferrer, C. C., Chen, M., Cucurull, G., Esiobu, D., Fernandes, J., Fu, J., Fu, W., Fuller, B., Gao, C., Goswami, V., Goyal, N., Hartshorn, A., Hosseini, S., Hou, R., Inan, H., Kardaş, M., Kerkez, V., Khabsa, M., Kloumann, I., Korenev, A., Koura, P. S., Lachaux, M.-A., Lavril, T., Lee, J., Liskovich, D., Lu, Y., Mao, Y., Martinet, X., Mihaylov, T., Mishra, P., Molybog, I., Nie, Y., Poulton, A., Reizenstein, J., Rungta, R., Saladi, K., Schelten, A., Silva, R., Smith, E. M., Subramanian, R., Tan, X. E., Tang, B., Taylor, R., Williams, A.,

- Kuan, J. X., Xu, P., Yan, Z., Zarov, I., Zhang, Y., Fan, A., Kambadur, M., Narang, S., Rodriguez, A., Stojnic, R., Edunov, S., and Scialom, T. Llama 2: Open foundation and fine-tuned chat models, 2023. URL <https://arxiv.org/abs/2307.09288>.
- Wang, J., Su, Y., Li, J., Xia, Q., Ye, Z., Duan, X., Wang, Z., and Zhang, M. Opt-tree: Speculative decoding with adaptive draft tree structure, 2024. URL <https://arxiv.org/abs/2406.17276>.
- Wang, Y., Ivison, H., Dasigi, P., Hessel, J., Khot, T., Chandu, K. R., Wadden, D., MacMillan, K., Smith, N. A., Beltagy, I., and Hajishirzi, H. How far can camels go? exploring the state of instruction tuning on open resources, 2023.
- Xiao, G., Lin, J., Seznec, M., Wu, H., Demouth, J., and Han, S. Smoothquant: Accurate and efficient post-training quantization for large language models. In *International Conference on Machine Learning*, 2023.
- Xiong, W., Shi, C., Shen, J., Rosenberg, A., Qin, Z., Candelriello, D., Khalman, M., Joshi, R., Piot, B., Saleh, M., Jin, C., Zhang, T., and Liu, T. Building math agents with multi-turn iterative preference learning, 2024. URL <https://arxiv.org/abs/2409.02392>.
- Yu, G.-I., Jeong, J. S., Kim, G.-W., Kim, S., and Chun, B.-G. Orca: A distributed serving system for Transformer-Based generative models. In *16th USENIX Symposium on Operating Systems Design and Implementation (OSDI 22)*, pp. 521–538, Carlsbad, CA, July 2022. USENIX Association. ISBN 978-1-939133-28-1. URL <https://www.usenix.org/conference/osdi22/presentation/yu>.
- Zhang, M., Press, O., Merrill, W., Liu, A., and Smith, N. A. How language model hallucinations can snowball. *arXiv preprint arXiv:2305.13534*, 2023.
- Zhao, J., Wan, B., Peng, Y., Lin, H., and Wu, C. Llm-pq: Serving llm on heterogeneous clusters with phase-aware partition and adaptive quantization, 2024a. URL <https://arxiv.org/abs/2403.01136>.
- Zhao, Y., Lin, C.-Y., Zhu, K., Ye, Z., Chen, L., Zheng, S., Ceze, L., Krishnamurthy, A., Chen, T., and Kasikci, B. Atom: Low-bit quantization for efficient and accurate llm serving, 2024b. URL <https://arxiv.org/abs/2310.19102>.
- Zheng, L., Chiang, W.-L., Sheng, Y., Li, T., Zhuang, S., Wu, Z., Zhuang, Y., Li, Z., Lin, Z., Xing, E., et al. Lmsys-chat-1m: A large-scale real-world llm conversation dataset. *arXiv preprint arXiv:2309.11998*, 2023.

## A Full Experiment Result.

### A.1 Acceleration Evaluation

#### Versus quantization configurations.

Table 7 presents the comprehensive comparison of token generation throughput across multiple dimensions: model sizes, quantization configurations, and batch sizes, evaluated on various datasets. It is noteworthy that Llama2-7B shows higher speedup than Llama3-8B. This stems from the size difference primarily related to vocabulary, coupled with the introduction of Group-Query Attention (Ainslie et al., 2023), reducing the computation workload.

**Versus speculative decoding.** Table 8 presents a comprehensive comparison between our approach and the EAGLE method across multiple benchmarks.

### A.2 Ablation Studies

#### Comprehensive Performance Trade-offs: QSpec versus W4A16

We conduct a thorough analysis of the trade-offs between throughput and accuracy for our proposed framework against all baseline implementations. Figure 7 illustrates this comparison, plotting generation quality (accuracy) against computational efficiency (throughput). Our analysis reveals that while W4A4 suffers substantial performance degradation (18.5-39.5% reduction) on multi-step reasoning benchmarks compared to W4A16, QSPEC achieves comparable accuracy to W4A16 while delivering significantly higher throughput. Although QSPEC’s accuracy is marginally lower than W16A16 due to weight quantization-induced memory optimization, it successfully preserves the performance characteristics of W4A16 while offering superior computational efficiency.

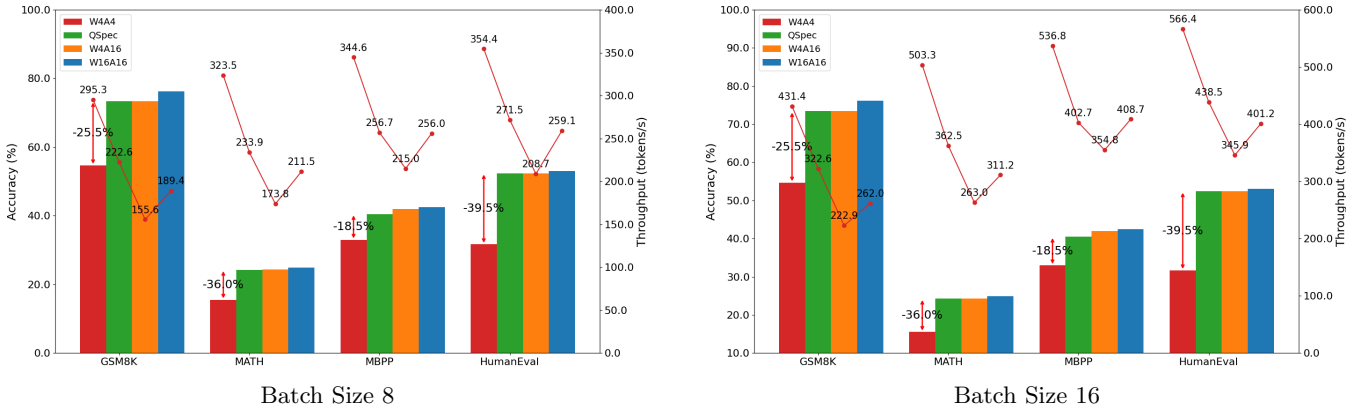


**Figure 7:** Comparison of accuracy and efficiency among W16A16, W4A16, W4A4, and QSPEC across various datasets with batch sizes of 8 and 16 on Llama3-8b-instruct model. The bars and lines represent the accuracy and throughput of each method.

### A.3 Datasets and Sampling

For the PIQA and Winogrande datasets, we randomly select 500 questions from each for performance evaluation. In contrast, we process the entire GSM8K and MATH datasets, as detailed in Atom Zhao et al. (2024b). When adapting QSPEC to the Quarot method, we sample 200 samples from the GSM8K dataset, while sampling 700 from the MATH dataset, ensuring balanced representation by selecting 100 questions from each of the seven distinct question types. Additionally, we sample 200 questions from the MBPP dataset, while processing the entire HumanEval dataset. This preserves a thorough assessment of the model’s performance across various datasets.

For acceleration evaluation, we maintain the random seed at 42, and sample 100 samples from the GSM8K, MATH, MBPP, HumanEval, ShareGPT, and LMSys datasets, respectively. This consistent methodology guarantees that our evaluation remains reproducible and representative across these diverse datasets.

## B Evaluation Datasets

We comprehensively evaluate the performance of QSPEC, covering language modeling, commonsense reasoning, mathematical reasoning, code and chatbot. Each dataset is briefly introduced below, along with the associated sampling strategy for enhanced efficiency.

**Table 7:** Comparison of token generation throughput across different model sizes, quantization configurations, and batch sizes for various datasets. All values are measured in token/s. “Avg.” denotes the average speedup ratio for the corresponding row or column. “†” indicates the failure of W4A16 kernels to support these batch sizes together with long sequences and the large models.

Model	Method	Batch	GSM8K	MATH	MBPP	HumanEval	ShareGPT	LMsys-1k	Avg.	
3B <sup>1</sup>	W16A16	8	511.1	588.7	756.6	647.2	785.7	711.2	–	
		16	666.5	845.6	1171.0	948.3	1292.2	1126.4	–	
		32	833.4	1081.5	1697.7	1111.6	1975.6	1553.3	–	
	W4A4	8	804.7	921.2	1002.0	892.6	1091.6	990.3	–	
		16	1109.1	1374.5	1548.0	1289.8	1763.5	1581.0	–	
		32	1424.3	1899.3	2300.6	1488.2	2777.3	2194.4	–	
	W4A16	8	420.0	476.7	604.5	535.7	610.4	559.8	–	
		16	578.5	715.9	989.7	804.4	1080.2	925.8	–	
		32	726.3	933.8	1536.7	954.4	1704.5	1336.4	–	
	QSPEC	8	594.1 (1.41×)	648.2 (1.36×)	760.1 (1.26×)	723.6 (1.35×)	787.5 (1.29×)	738.8 (1.32×)	1.33×	
		16	811.5 (1.40×)	936.0 (1.31×)	1157.8 (1.17×)	1042.1 (1.30×)	1294.5 (1.20×)	1171.4 (1.27×)	1.27×	
		32	1030.4 (1.42×)	1240.2 (1.33×)	1617.4 (1.05×)	1248.5 (1.31×)	1969.6 (1.16×)	1576.0 (1.18×)	1.24×	
		Avg.	1.41×	1.33×	1.16×	1.32×	1.21×	1.25 ×	1.28×	
	7B	W16A16	8	213.4	254.3	278.8	316.7	322.4	285.3	–
			16	290.3	362.1	447.7	505.1	541.3	441.6	–
32			340.9	441.6	585.3	663.6	735.3	564.2	–	
W4A4		8	349.5	411.7	396.1	471.2	471.8	419.4	–	
		16	496.6	612.2	614.3	749.5	760.9	642.6	–	
		32	620.0	793.6	801.5	1043.9	1083.2	865.5	–	
W4A16		8	165.0	193.1	224.5	240.2	243.5	220.2	–	
		16	231.8	286.5	384.4	407.3	435.9	358.0	–	
		32	268.9	359.9	480.0	555.9	620.2	470.1	–	
QSPEC		8	253.7 (1.54×)	291.5 (1.51×)	298.3 (1.33×)	350.9 (1.46×)	345.7 (1.42×)	310.3 (1.41×)	1.44×	
		16	359.8 (1.55×)	420.2 (1.47×)	466.7 (1.21×)	555.2 (1.36×)	557.8 (1.28×)	473.1 (1.32×)	1.37×	
		32	441.8 (1.64×)	527.2 (1.46×)	575.3 (1.20×)	749.4 (1.35×)	770.0 (1.24×)	628.4 (1.34×)	1.39×	
		Avg.	1.58×	1.48×	1.25×	1.39×	1.31×	1.36×	1.39×	
8B		W16A16	8	189.4	211.5	256.0	259.1	290.7	265.8	–
			16	262.0	311.2	408.7	401.2	511.0	447.4	–
	32		303.8	390.8	566.3	522.6	820.0	649.8	–	
	W4A4	8	295.3	323.5	344.6	354.4	395.9	366.8	–	
		16	431.4	503.3	536.8	566.4	697.5	621.1	–	
		32	532.8	688.5	755.7	763.7	1167.9	956.8	–	
	W4A16	8	155.6	173.8	215.0	208.7	231.1	215.6	–	
		16	222.9	263.0	354.8	345.9	422.8	369.4	–	
		32	†	†	509.8	468.7	706.0	580.5	–	
	QSPEC	8	222.6 (1.43×)	233.9 (1.35×)	256.7 (1.19×)	271.5 (1.30×)	285.0 (1.23×)	268.3 (1.24×)	1.29×	
		16	322.6 (1.45×)	362.5 (1.38×)	402.7 (1.14×)	438.5 (1.27×)	507.5 (1.20×)	453.5 (1.23×)	1.28×	
		32	400.2 (†)	362.5 (†)	578.1 (1.13×)	573.0 (1.22×)	798.8 (1.13×)	684.5 (1.18×)	1.27×	
		Avg.	1.44×	1.36×	1.15×	1.26×	1.19×	1.22×	1.27 ×	
	13B <sup>1</sup>	W16A16	8	121.9	146.6	183.1	182.0	187.1	160.1	–
			16	169.6	211.2	304.4	291.0	311.0	243.0	–
32			202.4	253.8	426.0	423.5	311.0	334.2	–	
W4A4		8	194.7	228.2	253.6	261.5	259.8	228.2	–	
		16	288.3	349.2	415.3	424.9	431.5	348.4	–	
		32	369.8	469.9	606.7	665.4	431.5	508.8	–	
W4A16		8	94.8	112.9	143.4	140.0	146.7	127.9	–	
		16	136.1	171.9	250.8	236.9	255.9	207.2	–	
		32	†	†	376.4	365.5	255.9	287.4	–	
QSPEC		8	148.2 (1.56×)	167.9 (1.49×)	193.6 (1.35×)	201.2 (1.44×)	194.5 (1.33×)	174.0 (1.36×)	1.42×	
		16	212.8 (1.56×)	248.6 (1.45×)	316.8 (1.26×)	323.3 (1.36×)	327.4 (1.28×)	266.9 (1.29×)	1.29×	
		32	266.6 (†)	320.0 (†)	451.5 (1.20×)	483.0 (1.32×)	327.4 (1.28×)	379.3 (1.32×)	1.32×	
		Avg.	1.56×	1.47×	1.27×	1.37×	1.29×	1.32×	1.38×	

**Table 8:** Performance comparison of EAGLE-Quant, QSPEC, W4A16, and W4A4 on Llama-2-7b-chat-hf across different batch sizes. Results are reported for GSM8K (8-shot), MATH (4-shot), MBPP (0-shot), HumanEval (0-shot), ShareGPT, and LMsyst-1k benchmarks. “OOM” indicates out-of-memory errors. Better case for QSPEC or EAGLE is marked in gray. In the case of batch size=8, the speedup ratio of QSPEC compared to EAGLE is indicated in parentheses next to the data points.

Method	Batch Size	GSM8K (8-shot)	MATH (4-shot)	MBPP (0-shot)	HumanEval (0-shot)	ShareGPT	LMsyst-1k
EAGLE	1	65.81	70.11	68.53	49.15	79.60	71.29
	8	140.16	210.52	138.01	136.86	247.42	167.57
	16	OOM	OOM	OOM	OOM	OOM	OOM
QSPEC	1	51.25	48.36	56.87	54.22	56.77	56.14
	8	208.95 (1.49×)	249.97 (1.19×)	185.13 (1.34×)	185.99 (1.36×)	329.44 (1.33×)	260.48 (1.55×)
	16	292.82	356.93	269.87	255.11	562.07	463.35
W4A16	1	59.80	63.65	75.49	72.04	76.04	72.27
	8	146.34	185.52	180.12	163.54	250.06	213.66
	16	190.09	251.59	254.24	211.49	458.57	371.38
W4A4	1	64.79	66.32	74.72	73.47	73.09	71.55
	8	284.84	369.27	250.11	256.54	492.21	393.12
	16	401.77	540.82	357.62	330.71	895.77	713.67

### Language Modeling and Commonsense Reasoning.

- **WikiText-2** (Merity et al., 2016): A language modeling dataset comprising over 100 million tokens extracted from high-quality Wikipedia articles.
- **PIQA** (Bisk et al., 2020): A benchmark for physical commonsense reasoning, focusing on questions about everyday physical interactions.
- **Winogrande** (Sakaguchi et al., 2019): A dataset of 44,000 problems inspired by the Winograd Schema Challenge, designed to test commonsense reasoning with reduced linguistic biases.

### Mathematical Reasoning

- **GSM8K** (Cobbe et al., 2021): A collection of 8,500 linguistically diverse grade school math problems that require multi-step reasoning using basic arithmetic operations.
- **MATH** (Hendrycks et al., 2021): A dataset of 12,500 challenging competition-level math problems, each accompanied by detailed step-by-step solutions.

### Code

- **MBPP** (Austin et al., 2021): A benchmark of approximately 1,000 beginner-level Python programming problems, each with a task description, solution code, and automated test cases.
- **HumanEval** (Chen et al., 2021): An evaluation set of 164 original programming problems used to assess functional correctness in code synthesis from docstrings.

### Chatbot

- **ShareGPT52K** (RyokoAI, 2021): This dataset comprises approximately 52,000 conversations collected via the ShareGPT API before it was discontinued. The dataset captures both user prompts and the corresponding responses from OpenAI’s ChatGPT, providing insights into human-AI dialogue dynamics.
- **LMsyst-chat-1M-1K** Zheng et al. (2023): Gathering one million authentic conversations with 25 leading large language models, this dataset was sourced from over 210,000 unique IP addresses interacting with the Vicuna demo and Chatbot Arena websites.

## C Datasets Sampling

To construct our test sets, we randomly sampled from the original datasets using `torch.sample` with a fixed seed of 42, and constructed them as prompt instructions following the Open-Instruct templates (Wang et al., 2023). The sample sizes for each dataset are as follows:

- **Fidelity Evaluation:**
  - **WikiText-2:** All samples
  - **PIQA:** 500 samples
  - **Winogrande:** 500 samples
  - **GSM8K:** 200 samples
  - **MATH:** 700 samples, balanced by selecting 100 questions from each of the seven distinct question types
  - **MBPP:** 200 samples
  - **HumanEval:** All samples
- **Acceleration Evaluation:** 100 samples from each dataset, maximum output length set to 200 tokens.